ELSEVIER

Journal of Nuclear Materials 313–316 (2003) 42–51

journal of nuclear materials

www.elsevier.com/locate/jnucmat

Material/plasma surface interaction issues following neutron damage

V. Barabash [a,*], G. Federici [a], J. Linke [b], C.H. Wu [c]

[a] *ITER International Team, Boltzmannstraße 2, 85748 Garching, Germany*
[b] *Forschungszentrum Juelich, EURATOM Association, 52425 Juelich, Germany*
[c] *EFDA Close Support Unit Garching, Boltzmannstraße 2, 85748 Garching, Germany*

Abstract

The main results of the effect of neutron irradiation on beryllium, tungsten and carbon based materials are summarized in the paper in terms of changes of the material's structure and physical and mechanical properties. As a consequence of the material property changes, some of the plasma-material interaction phenomena could change significantly. The effect on phenomena such as bulk tritium retention, behaviour during thermal transient events, and changes of the thermal conductivity are discussed. Based on the available data, the subsequent influence of the neutron irradiation on the performance of the plasma facing materials in ITER has been analysed. The performance of the plasma facing materials at higher neutron fluence (e.g. DEMO) is also discussed.

PACS: 50.40.Hf
Keywords: Plasma facing material; Defects; Thermal conductivity; Tritium retention; Thermal load

1. Introduction

The next step in the worldwide fusion program is the construction of a fusion experiment, ITER, with a burning reactor-scale D–T plasma. The selection of the plasma facing materials is one of the key issues due to the complexity of the operational conditions. In the reactor, the plasma facing materials will be subjected not only to energetic particles and high heat fluxes as in current facilities, but also to intensive neutron irradiation. Among the different possible plasma facing materials, beryllium, tungsten and carbon-based materials are under consideration [1].

The main physical and mechanical properties of these materials (Be, W, C) in unirradiated condition are well documented and could be found in the in various publications, e.g. in the ITER Materials Properties Handbook [2].

Neutron irradiation produces radiation-induced defects and changes of the microstructure which, in some cases, lead to a change in the chemical composition of the materials due to transmutation and, as a result, changes in physical and mechanical properties [3].

The degradation of the properties due to neutron irradiation could lead to significant changes in the materials–plasma surface interaction (PSI) phenomena. The main phenomena are damage during transient off-normal events (e.g. disruptions, vertical displacement events (VDEs)) and bulk tritium retention. Additionally, an important consequence of the neutron irradiation is the change of the physical properties (e.g. thermal conductivity for carbon-based materials), which must be taken into account during assessment of temperature-dependant mechanisms such as chemical sputtering of carbon.

This paper reviews the features related to PSI for beryllium, tungsten and carbon fibre composites following neutron irradiation. The consequence of the neutron irradiation for the ITER conditions (neutron

* Corresponding author. Tel.: +49-89 3299 4144; fax: +49-89 3299 4313/4163.
E-mail address: barabav@itereu.de (V. Barabash).

0022-3115/03/$ - see front matter
PII: S0022-3115(02)01330-2

fluence goal ~ 0.3 MWa/m^2) is analyzed in detail and the results presented. The further requirements and features of PSI for higher neutron fluence (e.g. DEMO reactor) are also discussed.

2. Neutron effect on structure and properties

It is well known that neutron irradiation leads to displacement damage of the lattice structure creating vacancies and interstitials, and to the generation of transmutation products. For armour materials (beryllium, tungsten and carbon), ferritic steel and vanadium alloys the values of radiation damage in displacement per atom (dpa) and transmutation elements production for the typical fusion spectrum with a neutron fluence of 1 MWa/m^2 are shown in Table 1.

It is known that dpa and transmutation are neutron fluence and spectrum dependent and also that the final structure of the irradiated material depends on irradiation temperature. The difference in the lattice damage under fusion and fission neutron spectra for materials such as Be, W and C has not been studied in the detail (as it has been done for structural materials). However, based on the results of simulations for pure materials such as Ni, Fe and Cu it has been concluded that the evolution of defects in cascades, the global defect accumulation and resulting microstructure changes, can be expected to be very similar [4].

The key difference is the transmutation production, which needs to be taken into account for the correct prediction of the material performance. A detailed assessment of the transmutation production in armour materials has been made [5]. Comparing these results with the results of irradiation in fission reactors, for beryllium, during irradiation in fission reactors, the typical value of the ratio (appm He/dpa) is 100–250, whereas for fusion neutron spectrum this value is $\sim$1000. For W, in the presence of the high energy neutrons in the fusion spectrum, there is a significant generation of solid products such as Re and Os. A similar rate of Re transmutation ($\sim$1–2 at.% Re/dpa) could be reached during irradiation in fast fission reactors, but for reactors with thermal neutron flux the Re generation is significantly lower [6]. For carbon, there is a peak reaction at neutron energies of 12 MeV, which leads to helium generation, with ratio (appm He/dpa) of $\sim$380. This helium generation by neutron irradiation in fission reactors could not be achieved.

These differences in the fission/fusion neutron spectra have to be taken into account when considering the structures of the irradiated materials and assessing the macro-performance of the materials at specific operational conditions (irradiation temperature, thermal transient events, etc.). For beryllium, depending on operational temperature, the dpa or He transmutation must be used as a reference neutron damage parameter. For low temperature irradiation ($\lesssim$300 °C) the dpa value must be considered. For high temperature irradiation ($\gtrsim$500 °C) the He generation must be taken as the reference parameter [7]. For carbon, it is known that He release starts at room temperature due to the high mobility in the hcp carbon lattice, [8]. This means that, for the typical operational temperatures range $\sim$200–1500 °C, the presence of He in materials could be ignored and does not affect the formation of the damaged structure. For W, the solid transmutation production (mainly Re) must be taken into account, especially at high irradiation fluences.

As seen from Table 1, a significant amount of tritium could be generated in beryllium during neutron irradiation. Tritium is produced in beryllium primarily by an n,α reaction with ^{8}Be to produce ^{6}He that rapidly decays to ^{6}Li. The ^{6}Li subsequently reacts with another neutron to produce both helium and tritium. This gives additional cause for concern on global tritium retention in armour materials in fusion reactors and must be taken into account.

3. Beryllium

3.1. Change of properties

Thermal conductivity: Recently several studies have been carried out to investigate the effect of neutron irradiation on the thermal conductivity of beryllium. For S-65C Be grade irradiated up to 10^{21} n/cm^2 ($\sim$0.74 dpa)

Table 1
Damage and transmutation productions for different materials for a neutron fluence of 1 MWa/m^2

Material	dpa	He (appm)	H, D, T (appm)	Others (%)
Be	3.5	3500	$\sim$50 (T)	–
C	4.5	1500	0.2	–
W	3.5	2	0.1	Re: 3, Ta: 0.8, Os: 0.2
Ferritic steel	8.3	150	300	Reducing of W, some Re, Os
V	8.5	50	160	–

at ~300 °C the thermal conductivity was within experimental error of the unirradiated value, [9]. No effect was seen for Be S-65C after irradiation at 350 and 700 °C at a damage dose ~0.35 dpa [10].

For Be S-200F grade irradiated at 200 °C up to fluence 4.5×10^{21} n/cm^2 ($E > 1$ MeV, 88 appm He and ~0.6 dpa), the thermal conductivity of irradiated Be decreased to about 90% of the original value [11]. After high temperature annealing, in specimens with 29% and 63% swelling, thermal conductivity decreased to about 70% and 40% of that of unirradiated material, respectively.

A significant change of the thermal conductivity beryllium (TE-56 grade, Russian Federation) was observed after irradiation at a temperature 70 °C and damage dose of ~32 dpa. In this case thermal conductivity was reduced from ~200 to ~35 W/mK at ambient temperature [12]. Post irradiation annealing of beryllium at a temperature of 500 °C during 1 h leads to the partial recovery of the initial thermal conductivity to a level of ~110–140 W/mK. However, at higher irradiation temperatures ~400 °C and much higher fluence (~94 dpa), the thermal conductivity for grade TE-400 was reduced only from 180 to 150 W/mK.

It could be concluded that at conditions which lead to significant changes of the beryllium structure, such as the formation of a high density of radiation defects (especially at low irradiation temperature and high dose) or high swelling, significant changes in the thermal conductivity could take place. This must be included in the detailed assessment of the performance of beryllium armour.

Swelling: It is well known that beryllium swell when irradiated by neutrons, especially during high temperature irradiation. A comprehensive review of the swelling data for different Be grades and the proposed empirical correlations has been recently made [3,13]. For prediction of Be swelling the ANFIBE code could be used [14]. The driving force for the swelling is the presence of He, which forms He bubbles, especially during high temperature irradiation ($\gtrsim$ 400 °C) or after high temperature annealing. The maximum values of swelling could reach values of ~ tens of percent. However, the swelling depends on the structure of the beryllium: beryllium grades with small grain size (~8–10 μm) and high BeO content (~3–4 wt%) have a higher resistance to swelling than conventional Be grades [3].

Mechanical properties: Neutron irradiation typically leads to degradation of the ductility of beryllium [3]. The main concern is the embrittlement of Be at low irradiation temperature ($\lesssim$ 200 °C) due to accumulation of the radiation defects in the form of dislocation loops, and at high irradiation temperature ($\gtrsim$ 400 °C) due to He bubble formation at grain boundaries. For the temperature range 240–480 °C and damage level ~1 dpa, it is expected that the ductility of Be will be at the level $\lesssim$ 1%.

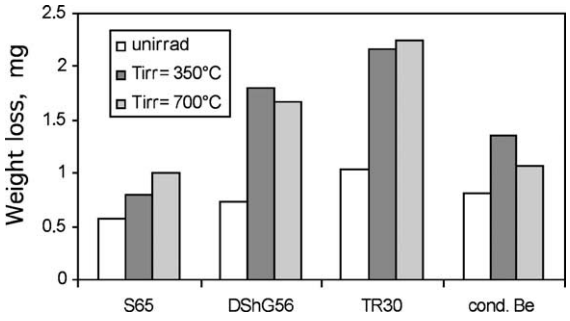

Fig. 1. Weight loss after thermal shock (15 MJ/m^2, 5 ms) of different neutron irradiated beryllium grades.

3.2. Thermal shock effect

Beryllium as armour could be subjected to thermal shocks (disruptions, VDEs). The damage during these events is a complex function of the heat flux parameters and material properties, which, as described above, are neutron irradiation dependent. Only limited studies of this effect have been performed [15,16]. The weight losses after such thermal shock for different grades of beryllium (irradiated at 350 and 700 °C, damage dose ~0.35 dpa) for a disruption load of ~15 MJ/m^2 are presented in Fig. 1. An increase of erosion after neutron irradiation (up to 100%) was observed. The main conclusion is that thermal erosion is not simple evaporation, but also could be the loss of some particles due to the brittle destruction of the surface. The embrittlement of the Be due to neutron irradiation increases the loss of material particles, especially at low irradiation temperature. A clear pore formation (which is expected to be He filled) has been observed in the melt layer of all neutron irradiated specimens after thermal shock loading.

3.3. Bulk tritium retention

The main source of the bulk tritium retention in beryllium armour is transmutation generation during neutron irradiation. These tritium atoms will be trapped by neutron-induced defects such as dislocation loops and helium bubbles. Bulk tritium retention due to implantation, and, as a result, the effect of the damaged structure on this retention, is expected to be less serious than previously anticipated [17]. The possible reason is the formation of surface-connected porosity that provides a rapid return path back to the plasma.

Several studies have directly demonstrated that neutron irradiated Be traps much more tritium compared to unirradiated material [18,19]. Tritium loading in these experiments has been performed by exposure to tritium in the gaseous phase. The main results were:

- in S-200E Be (irradiated at 40–50 °C and after a fluence of 4×10^{22} n/cm^2 or 40 dpa) the tritium retention increased with neutron fluence by a factor 10;
- in S-200 HIP Be after irradiation at 235–600 °C and ~1.5–1.7 dpa the bulk retention increased by a factor of 3.

Useful information has been generated in tritium release experiments using neutron irradiated material [20–24]. The main findings of these experiments are as follows:

- At temperatures $\lesssim$ 500 °C no tritium release was observed (for materials irradiated over wide fluence and temperature ranges).
- The release of tritium starts at ~600–700 °C. At this temperature typically ~10% of the tritium contained in the material is released. To release all tritium a temperature of ~900–1000 °C is required.
- At high temperature (>800 °C) tritium and helium are released concurrently and in burst-type manner due to microcrack formation in brittle irradiated material.
- At low irradiation temperature (<200 °C) tritium is trapped by defects and during heating is more easily released at 700–800 °C compared with high temperature irradiation, where tritium is in He bubbles.
- After high neutron fluence, release starts at lower temperature and is much faster than for weakly irradiated material.
- The apparent diffusion coefficient depends on the grain size: for the larger-grained specimens, the diffusion coefficient is greater than for small-grained specimens.

Summarizing the results, it can be concluded that all tritium will remain in the neutron-irradiated Be structure if the temperature of the material is kept lower than ~500 °C.

4. Carbon-based materials

4.1. Change of properties

Thermal conductivity: It is well known that neutron irradiation effects the thermal conductivity of the carbon-based materials [3,25,26]. The main reason is the formation of the radiation defects, which act as obstacles for the phonon propagation. The size and concentration of the radiation defects depends on irradiation temperature and fluence and, as a result, the thermal conductivity also depends on these parameters. The main features of this effect can be summarized as follows:

- The level of degradation of thermal conductivity significantly depends on irradiation temperature. Recently, the data after irradiation at 90 °C at damage doses in the range 0.002–0.13 dpa were generated [27]. The thermal conductivity of CFC SEP NB31 decreased from ~350 W/mK in unirradiated condition to ~6 W/mK after irradiation to a damage dose ~0.13 dpa. An increase of the irradiation temperature leads to a decrease of the degradation of the thermal conductivity, and above an irradiation temperature ~1500 °C there is no effect of neutron irradiation.
- An increase of the neutron fluence leads to a decrease in the thermal conductivity. Saturation in the thermal conductivity change has been observed. A decrease of the irradiation temperature decreases the saturation dose and the value of the normalized thermal conductivity K_{irr}/K_o.
- Thermal conductivity of irradiated CFCs may be partially restored by high temperature annealing and the level of the thermal conductivity recovery depends on the annealing temperature and neutron fluence.

The available data for neutron-irradiated CFCs has been collected. Based on this data an empirical equation describing the thermal conductivity changes for a wide range of neutron fluences and irradiation temperatures has been proposed for the calculation of the thermal performance of CFC-armoured components [28]. Fig. 2 shows the calculated thermal conductivity of CFC SEP NB31.

Dimensional stability: Neutron irradiation leads to formation of the displaced carbon atoms, which form the dislocation loops and additional graphite planes at

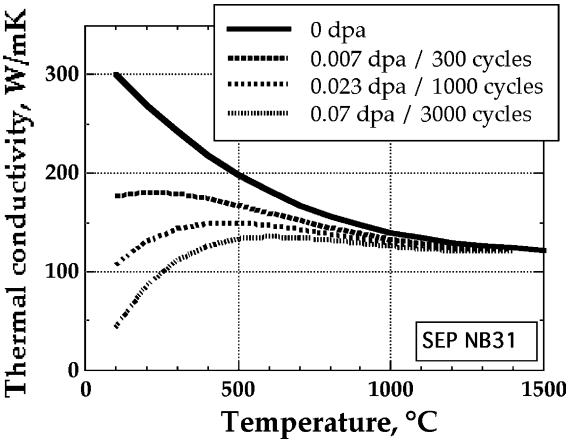

Fig. 2. Calculated thermal conductivity of the CFC SEP NB31 as a function of irradiation temperature and neutron damage.

specific irradiation conditions. These cause the extension of the graphite crystal in the $\langle c \rangle$ direction [29]. The dimensional changes of CFCs are a function of neutron dose and irradiation temperature. The type of fibers and architecture of the composites also play important role determining the dimensional stability. Dimensional changes in 2D and 3D materials are more isotropic in comparison with 1D CFCs. Turnaround to growth (which determines the maximum irradiation dose for carbon based materials) for 1D and 2D CFCs appeared earlier than in 3D CFCs. For the irradiation temperatures ~300–1200 °C and damage dose ~0.1 dpa the dimensional change (shrinkage) is $\lesssim$ 0.1–0.2%.

Mechanical strength, coefficient of thermal expansion and elastic modulus: Neutron irradiation increases the Young's modulus and the strength, with some reduction of the ductility. A change as high as ~30–40% is expected for a fluence of ~1 dpa at an irradiation temperature in the range of 300–1200 °C. The data for the thermal expansion coefficient shows no significant dependence on irradiation, and the expected changes are with ~25% of unirradiated values [29].

4.2. Thermal shock effect

The behaviour of neutron irradiated CFCs at specific conditions simulating thermal shocks and disruptions has been studied recently [30,31]. CX 2002U was irradiated at 290–320 °C and a fluence up to 5.6×10^{20} n/cm^2 (~0.5 dpa), and after irradiation the samples were subjected to thermal shock (500–800 MW/m^2, 25–40 ms) [30]. The measured thermal erosion was ~ twice as high as the thermal erosion of the unirradiated material. The main reason is the reduction of the thermal conductivity by irradiation.

Similar tests were performed [31]: CFCs such as NS11, NB31, Dunlop and CX 2002U were irradiated at 350 and 750 °C to a damage level ~0.3, dpa and thermal shock tests were carried out at 8.4 MJ/m^2. Generally, the thermal erosion of materials irradiated at 350 °C was higher than the erosion of unirradiated CFCs and CFCs irradiated at 750 °C. This can again be explained by a reduction of the thermal conductivity due to neutron irradiation.

4.3. Bulk tritium retention

Tritium retention in irradiated carbon based materials has been reported extensively [18,22,32–40]. This effect has been also recently reviewed [41]. Due to the generation of radiation defects, neutron irradiation leads to an increase the number of traps. The main trap sites are the edge carbon atoms of interstitial loops, and edge carbon atoms at grain surfaces. The main findings could be summarised as follows:

- neutron irradiation leads to an increase in the solubility of tritium in carbon-based materials by a factor ~20–50;
- depending on irradiation temperature, the tritium retention saturates at a damage dose ~0.04–0.3 dpa;
- the tritium trap density depends on irradiation temperature – increase of the temperature reduces the level of radiation damage and, consequently – trap density;
- bulk tritium retention in CFCs is significantly lower in comparison with graphite.

Recent results of tritium release experiments from neutron irradiated CFCs have been presented [22,40]. Several CFCs were irradiated at 335 °C/0.31 dpa and 775 °C/0.35 dpa and tritium was loaded at 0.2 MPa at 850 °C. The main results were

- for all materials (carbon and CFCs) tritium release at temperatures $\lesssim$700 °C was not observed, the maximum release rate is at temperatures of ~1100 °C;
- tritium retention decreases with an increase of the irradiation temperature, saturation was observed at ~0.1 dpa and the trap density was ~1000 appm;
- the behaviour of Si-doped CFC is the same as for undoped materials;
- annealing of irradiated CFC before exposure at 1300 °C decreases the tritium retention by several time which confirms that traps are radiation-induced.

5. Tungsten

5.1. Change of properties

Thermal conductivity: There is no direct data on the effect of irradiation on the thermal conductivity of tungsten. The maximum increase of electrical resistance of 24% was measured in pure W after irradiation to about 4 dpa [3]. In accordance with the Wiedemann–Franz law, the electrical resistance of metals is inversely proportional to thermal conductivity, so the latter should change accordingly. However, at higher neutron fluence, significant generation of Re is expected and due to this the thermal conductivity should be reduced. The thermal conductivity of the W–5%Re is ~80% of pure W and increase of Re will further reduce the thermal conductivity.

Swelling: A summary of the swelling data for W has been made [3]. The maximum reported swelling was ~1.7% at 9.7 dpa and 800 °C. However, a significant change of the microstructure is observed in tungsten, mainly the formation of a superlattice of voids. For instance [42], a superlattice of voids with diameter ~20 nm and lattice parameter ~120 nm was observed after irradiation at 550 °C at neutron damage ~7 dpa (Fig. 3).

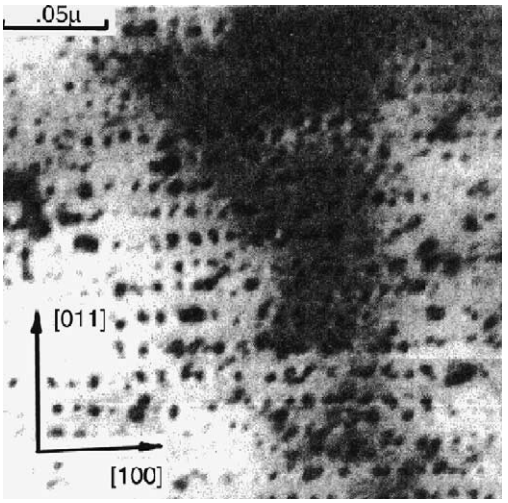

Fig. 3. Ordered array of voids in W irradiated at 550 °C at neutron fluence $\sim 10^{22}$ n/cm^2 ($\sim$7 dpa).

The presence of this type of defect is very important for the assessment of bulk tritium retention.

Mechanical properties: W becomes brittle after neutron irradiation due to radiation hardening and loss of strength at grain boundaries which lead to an increase in the ductile-to-brittle transition temperature (DBTT), [3]. This effect depends mainly on irradiation temperature. At low irradiation temperatures ($\lesssim$ 500 °C) and damage $\sim$ tens of dpa the DBTT increases up to $\sim$500–700 °C. There is some hope that at irradiation temperatures $\gtrsim$ 900 °C, the DBTT of W will remain unchanged, but it should be further demonstrated. There is also preliminary data showing that W with small TiC strengthening particles could be more radiation resistant compared to pure unalloyed W, [43], but still some further development is needed.

5.2. Thermal shock effect

Several grades of tungsten (W–1%La_2O_3, W–5%Re and plasma-sprayed W) have been irradiated in the Paride 1 and 2 program (damage dose $\sim$0.3 dpa, irradiation temperature $\sim$350 and 700 °C) [44] and then exposed in the Judith facility to high thermal heat fluxes. At the maximum energy densities available in the Judith facility ($\lesssim$ 20 MJ/m^2), the weight losses for irradiated and unirradiated materials were very similar. Crack formation was observed similar to that of the unirradiated materials. No significant influence resulting from neutron irradiation has been observed so far.

Crack formation in W during thermal shock tests could be reduced if the initial temperature of the samples is higher than the DBTT. This has been confirmed for unirradiated W, (Fig. 4), and also could be expected for irradiated material. This result shows that keeping the surface temperature of W higher than $\sim$900 °C is beneficial for the reduction of crack formation.

5.3. Bulk tritium retention

Due the high activation of W there is no direct data on the effect of neutron irradiation on bulk tritium retention. However, from the available data for unirradiated W (see as example review [41]) and comparing the structure of the studied materials with neutron irradiation, some preliminary conclusion can made. Trapping of hydrogen can take place at many sites within materials, such as dislocation loops, voids, grain, and phase boundaries. The structure of the neutron irradiated W depends on irradiation temperature and fluence. At low irradiation temperature ($\lesssim$ 400 °C) the structure consist of small dislocation loops with diameter $\sim$5–20 nm with density $\sim 0.01–1 \times 10^{23}$ m^{-3} and the density saturates at a damage dose $\sim$10 dpa, [45]. At moderate temperature, the formation of the small vacancy voids occurs. During irradiation, Re generation will take place. At low and moderate temperatures Re remains in solid solution, but at high temperature the formation of the Re-rich Sigma- and chi-phases occurs.

Among the available results, the data for unirradiated W, which gives a correlation between the structure and tritium retention, could be used to make the preliminary recommendations. Tritium retention in W

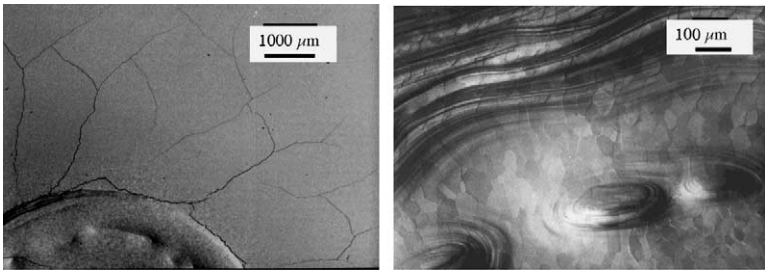

Fig. 4. Surface structure of the W samples after thermal shocks, 2.3 MJ/m^2, 1.8 ms, 10 shots: (a) initial temperature – RT and (b) initial temperature – 650–700 °C.

samples with different dislocation densities has been studied [46]. In as-received W, the dislocation density was $\sim 1.3 \times 10^{14}$ m^{-2} in grains and $\sim 10^{15}$ m^{-2} in cell walls. After annealing at 1400 °C the total dislocation density was reduced by ~7 times. As a result of this structure change the trap density in annealed W was ~7 times lower. Taking into account that during low temperature irradiation the presence of dislocation loops increases the total dislocation density to 10^{15}–10^{16} m^{-2}, the expected tritium retention in this material would be significantly higher than in typical W.

For W with a different phase structure, the bulk tritium retention could also be different [47]. Pure W and W–1%La_2O_3 were exposed to 100 eV tritium at ~50–700 °C. The retention reached a maximum at ~320 °C for pure W and ~420 °C for doped material and the maximum retention in W–1%La_2O_3 was twice as high as higher with pure W. This result demonstrates that the presence of the additional phases, especially grain boundaries, could play a significant role in bulk tritium retention.

The interaction of the hydrogen isotopes with voids in W has been studied [48]. Voids were created by the irradiation with 30 keV deuterium ions and were observed at irradiation temperature higher than ~300 °C, which is generally not typical for neutron-generated voids. Upon annealing, the release of deuterium occurred at ~300–500 °C.

Depending on the design of the plasma facing components, W armour will have a different microstructure (reflecting the irradiation temperature) and this make the assessment of the total bulk retention very complicated.

6. Key issues for ITER

ITER is planned to be the first fusion reactor with significant fusion neutron fluence of ~0.3 MWa/m^2. The selection and the performance of the armour materials in ITER (Beryllium for the first wall, tungsten and CFC for the divertor), including the effect of neutron irradiation, have been discussed extensively in several ITER documents and publications [28,49,50]. Neutron irradiation under ITER conditions leads to a change of the properties of the armour materials as has been described. Some of these changes are very important for performance, and some are not so significant. For each ITER armour material the PSI issues will be discussed below.

Beryllium: The maximum expected neutron damage is ~1.5 dpa, 1500 appm He, and the operation temperature for the first wall is ~200–300 °C (for the limiter the maximum temperature during start up ~700 °C). Due to the low fluence the expected change of thermal properties is negligible. There are two main issues for Be armour related to the effect of neutron on PSI.

The first is the damage during transient events such as VDEs and disruptions. Neutron irradiation leads to increase of the thermal erosion due to the destruction of the embrittled beryllium [15,16]. This effect was taken into account in the selection of the beryllium thickness. Still more data are needed under more relevant conditions, especially regarding He content.

The second is the bulk tritium retention due to transmutation. Based on the available data, the tritium inventory in the beryllium first wall due to implantation, diffusion, trapping and neutron-induced transmutation, after 12 000 pulses, will be of the order of 20 g (most of which comes from breeding reactions). Tritium retention in n-induced traps could increase this inventory somewhat (e.g., up to ~90 g for a trap density of 0.1 at.% and 250 g for high trap density of 1 at.% and trap energy of 1.4 eV) [49]. Taking into account that the majority of the ITER first wall will be kept at temperature $\lesssim$ 300 °C, all bread tritium will be retained in the beryllium. Partially this tritium will be released with eroded beryllium. It is still not accurately known how much tritium will permeate deeper into the beryllium and what will be the effectiveness of the neutron traps. Therefore, experiments are needed to determine the depth dependence of tritium concentration in the bulk material and to examine the effect of radiation damage on the tritium retention.

Tungsten: The neutron damage is ~0.1 dpa (taking into account the replacement of the divertor cassette) and operational temperature ~200–1300 °C. The generation of solid transmutation products is small due to the low expected fluence and the expected change of thermal properties is negligible. There is no neutron effect on behaviour during transient events, at least for these conditions. Due to the low fluence, radiation damage structure such as dislocation loops do not increase significantly the total dislocation density, which is critical for the bulk retention. No void formation is expected at these conditions.

Carbon fibre composites: The expected neutron damage is $\lesssim$ 0.1 dpa, and the operational temperature range is ~200–1500 °C. As was shown, neutron damage could increase the thermal erosion due to transient events, but taking into account the low damage dose and high surface temperature during disruptions, this increase will be very minor in comparison with the total erosion during disruptions and ELMS. The bulk tritium retention due to the generation of the radiation defects caused by neutron irradiation will increase, but in any case it will be significantly lower than tritium retention in codeposited layers [49].

Neutron irradiation at this low fluence will cause rapid deterioration in the thermal conductivity of C, and this will lead to a change of the temperature along the target for a given thickness and heat flux. This temperature change will in turn lead to a change of chemical

erosion. Chemical erosion for carbon is a complicated process that depends on particle energy and flux, surface temperature and material properties such as crystalline structure [51]. In ITER, chemical erosion is predicted to dominate the erosion of the vertical target during normal operation conditions and gross and net erosion rates are higher in the detached portion of the plasma near the separatrix [52].

A simplified analysis to predict this effect has being carried out for the ITER divertor using a typical background plasma solution produced by B2-EIRENE [50], which provides the particle and heat fluxes along the PFC surfaces. The change of the surface temperature profile resulting from neutron irradiation for three different irradiation times and a constant target thickness is plotted in Fig. 5 for the inner (maximum heat flux 5 MW/m^2) and outer target (maximum heat flux 10 MW/m^2) of the ITER divertor for SEP NB31 CFC. The resulting changes of the gross chemical erosion calculated with the formula of Roth [53] are plotted in Fig. 6. The effect seems to be marginal and the effect of the change of the thermal conductivity is not so important. However, a more detailed analysis is needed.

7. Step after ITER

For DEMO and for commercial fusion reactors the problems of the effect of neutron irradiation on materials became more and more important and this could have a significant effect on the design and selection of the armour materials. Several concepts of future reactors are under evaluation nowadays. The most promising armour material is W for the divertor and first wall. Unarmoured first wall designs are also under consideration. Beryllium and carbon have been eliminated from the list of candidates due to high erosion rate and high tritium retention [1]. Liquid metals are also under considerations [41].

For W armour it is important to understand the effect of high neutron dose (~30–50dpa, which creates ~30%

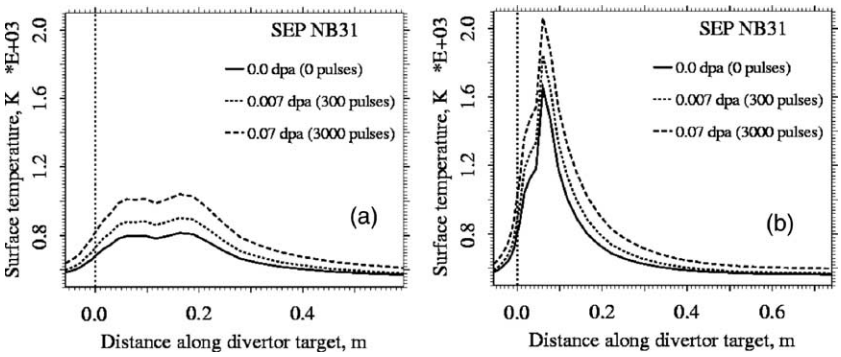

Fig. 5. Calculated temperature distribution along the ITER (a) inner divertor target and (b) outer divertor target at different irradition times: after (1) 0 pulses (0 dpa); (2) 300 pulses (0.007 dpa); and (3) 3000 pulses (0.07 dpa), for an assumed constant thickness of the target of 20 mm.

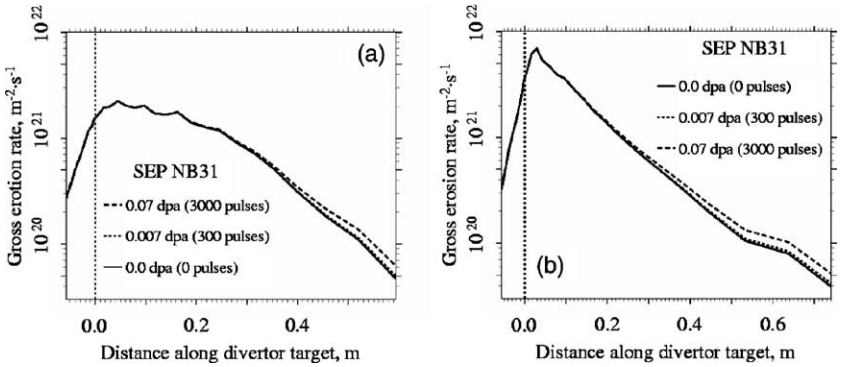

Fig. 6. Calculated chemical erosion rates (gross erosion) along the ITER (a) inner divertor target and (b) outer divertor target at different irradition times: after (1) 0 pulses (0 dpa); (2) 300 pulses (0.007 dpa); and (3) 3000 pulses (0.07 dpa), for an assumed constant thickness of the target of 20 mm.

of Re) on the bulk tritium retention. This is important for the selection of the operation window for W armour and for the selection of the design of divertor and first wall.

Using unarmoured first wall materials (low activation ferritic steel or vanadium alloys) has some advantages such as simplicity of the design, higher tritium breeding ratio, etc. However, the key issues for these materials are bulk tritium retention and permeation, especially at high neutron dose (~100 dpa) and simultaneous neutron irradiation. Both materials have extremely high interaction ability with hydrogen and mechanical properties could change significantly due to hydrogen embrittlement. Several studies have been performed to understand the interaction of hydrogen with ferritic steel [54,55] and with vanadium alloys [56–59]. However, results at high neutron fluence are still needed to justify the selection of an unarmoured first wall especially at high neutron fluence.

8. Conclusions

Changes in armour material properties under neutron irradiation have an impact on the PSI phenomena, in particular bulk tritium retention, behaviour under thermal transients (VDEs, disruptions). The change of the material thermal properties leads to a change of the surface temperature and as a result to a change of temperature-dependent processes such as e.g. chemical erosion.

Based on the available data, the effect of neutron irradiation on the performance of the armour materials (Be, W and C) for ITER has been summarized. Despite of the changes of material properties, neutron irradiation does not lead to a deterioration of the performance of the armour materials. However, a number of issues require the further confirmation by R&D for ITER. These include the behaviour of Be armour at relevant neutron damage during thermal transient events, features of the bulk tritium retention, and the nature of the traps in W and Be.

For reactors (DEMO, commercial) the issues related to neutron irradiation became more important. For the high neutron fluence expected in these projects, the PSI issues have not been studied and focused R&D has to be performed.

All present data related to consequent tests, for example first neutron irradiation and then specific PSI tests. However, in a reactor, the effects will occur simultaneously. For some phenomena, (e.g. permeation) this is important and has to be studied in the future.

Acknowledgements

This report was prepared as an account of work undertaken within the framework of ITER Coordinated Technical Activities (CTA). These are conducted by the Participants: Canada, the European Atomic Energy Community, Japan, and Russian Federation, under the auspices of the International Atomic Energy Agency. The views and opinions expressed herein do not necessarily reflect those of the Participants to the CTA, the IAEA or any agency thereof. Dissemination of the information in this paper is governed by the applicable terms of the former ITER EDA Agreement.

References

[1] H. Bolt, V. Barabash, G. Federici, et al., J. Nucl. Mater. 307–311 (2002) 43.
[2] ITER Materials Properties Handbook, ITER Document G 74 MA 9 01-07-11 W 0.2, July 2001.
[3] V. Barabash, G. Federici, M. Roedig, L.L. Snead, C.H. Wu, J. Nucl. Mater. 283–287 (2000) 138.
[4] S.J. Zinkle, J. Nucl. Mater. 307–311 (2002) 192.
[5] R. Behrisch, V. Khripunov, R.T. Santoro, J.M. Yesil, J. Nucl. Mater. 258–263 (1998) 686.
[6] L.R. Greenwood, F.A. Garner, J. Nucl. Mater. 212–215 (1994) 635.
[7] D. Gelles et al., J. Nucl. Mater. 212–215 (1994) 29.
[8] R.A. Langley, R.S. Blewer, J. Roth, J. Nucl. Mater. 76&77 (1978) 313.
[9] L.L. Snead, Fusion Materials Semiannual Progress Report, Period ending 30 June 1998 DOE/ER-0313/24, p. 215.
[10] M. Roedig, Final report ITER Task T221/1 (GB5), Report of FZ Juelich, IWV2-TN-3/2000, 20.09.00.
[11] E. Ishitsuka, H. Kawamura, T. Terai, S. Tanaka, in: C. Varandas, F. Serra (Eds.), Fusion Technology 1996, vol. 2, Elsevier, Amsterdam, 1997, p. 1503.
[12] D.N. Syslov, V.P. Chakin, R.N. Latypov, J. Nucl. Mater. 307–311 (2002) 664.
[13] D. Gelles et al., J. Nucl. Mater. 212–215 (1994) 29.
[14] M. Dalle Done, F. Scaffidi-Argentina, C. Ferrero, C. Rocci, in: Proceedings of the 1st Workshop on Beryllium Technology for Fusion, KFZ report 52711, 1993, p. 105.
[15] M. Roedig, R. Conrad, H. Derz, R. Duwe, J. Linke, A. Lodato, M. Merola, G. Pott, G. Vieider, B. Wiechers, J. Nucl. Mater. 283–287 (2000) 1161.
[16] J. Linke et al., J. Nucl. Mater. 290–293 (2001) 1102.
[17] G. Federici, J.P. Coad, A.A. Haasz, G. Janeschitz, N. Noda, V. Philipps, J. Roth, C.H. Skinner, R. Tivey, C.H. Wu, J. Nucl. Mater. 283–287 (2000) 110.
[18] K. Kwast, H. Werle, C.H. Wu, Phys. Scr. T 64 (1996) 41.
[19] C.H. Wu, J.P. Bonal, H. Kwast, et al., Fusion Eng. Des. 39&40 (1998) 263.
[20] D.L. Baldwin, M.C. Billone, J. Nucl. Mater. 212–215 (1994) 948.
[21] D.V. Andreev et al., J. Nucl. Mater. 233–237 (1996) 880.
[22] F. Scaffidi-Argentina, C. Sand, C.H. Wu, J. Nucl. Mater. 290–293 (2001) 211.
[23] E. Ishitsuka, H. Kawamura, T. Terai, S. Tanaka, M. Uda, in: B. Beaumont, P. Libeyre, B. de Gentile, G. Tonon (Eds.), Fusion Technology 1998, vol. 2, 1998, p. 1281.
[24] E. Ishitsuka et al., J. Nucl. Mater. 258–263 (1998) 566.

[25] V. Barabash, M. Akiba, J.P. Bonal, et al., J. Nucl. Mater. 258–263 (1998) 149.
[26] T. Burchell, T. Oku, J. Nucl. Fusion 5 (Suppl.) (1994) 79.
[27] V. Barabash, I. Mazul, R. Latypov, A. Pokrovsky, C.H. Wu, J. Nucl. Mater. 307–311 (2002) 1300.
[28] ITER Materials Assessment Report, ITER Document G 74 MA 10 01-07-11 W 0.2, July 2001.
[29] T. Burchell, T. Oku, Materials properties data for fusion reactor plasma-facing carbon–carbon composites, Nuclear Fusion 5 (Suppl.) (1994) 77.
[30] M. Uda, E. Ishitsuka, K. Sato, M. Akiba, et al., in: Proceedings of the SOFT-20, Marseille, September 1999, p. 161.
[31] M. Rödig, R. Conrad, H. Derz, R. Duwe, J. Linke, A. Lodato, M. Merola, G. Pott, G. Vieider, B. Wiechers, J. Nucl. Mater. 283–287 (2000).
[32] C.H. Wu, J.P. Bonal, H. Kwast, et al., Fusion Eng. Des. 39&40 (1998) 263.
[33] R. Causey, W. Harbin, D. Taylor, L. Snead, Phys. Scr. T 64 (1996) 32.
[34] W.R. Wampler, B.L. Doyle, R.A. Causey, K. Wilson, J. Nucl. Mater. 176&177 (1990) 983.
[35] R.A. Causey, K. Wilson, W.R. Wampler, B.L. Doyle, Fusion Technol. 19 (1991) 1585.
[36] H. Atsumi, I. Iseki, T. Shikama, J. Nucl. Mater. 191–194 (1992) 368.
[37] H. Atsumi et al., J. Nucl. Mater. 212–215 (1994) 1478.
[38] V. Chernikov et al., J. Nucl. Mater. 217 (1994) 250.
[39] K. Kwast et al., J. Nucl. Mater. 212–215 (1994) 1472.
[40] C.H. Wu et al., Fusion Eng. Des. 56&57 (2000) 179.
[41] R.A. Causey, J. Nucl. Mater. 300 (2002) 91.
[42] V.K. Sikka, J. Moteff, J. Appl. Phy. 43 (2) (1972) 4942.
[43] H. Kirishita, J. Nucl. Mater., these Proceedings.
[44] M. Rödig, R. Conrad, H. Derz, et al., J. Nucl. Mater. 283–287 (2000) 1161.
[45] V.V. Scherak, Fizika I Khimija Obrabotki Materialov, N 2 (1988) 6 (in Russian).
[46] R.A. Anderl, D.F. Holland, G.H. Longhurst, et al., Fusion Technol. 21 (1992) 745.
[47] R.A. Causey, K. Wilson, T. Venhaus, W.R. Wampler, J. Nucl. Mater. 266–269 (1999) 467.
[48] H. Eleveld, A. van Veen, J. Nucl. Mater. 212–215 (1994) 1421.
[49] G. Federici et al., Phys. Scr. T 91 (2001) 76.
[50] G. Federici et al., J. Nucl. Mater., these Proceedings.
[51] G. Federici, C.H. Skinner, et al., Nucl. Fusion 41 (2001) 1967.
[52] G. Federici et al., J. Nucl. Mater. 266–269 (1999) 14.
[53] J. Roth, J. Nucl. Mater. 266–269 (1999) 51.
[54] P. Jung, J. Nucl. Mater. 258–263 (1998) 124.
[55] S. Hara, J. Nucl. Mater. 258–263 (1998) 1280.
[56] K. Aoyagi et al., J. Nucl. Mater. 283–287 (2000) 876.
[57] V.L. Arbuzov et al., J. Nucl. Mater. 233–237 (1995) 442.
[58] Y. Hirohata et al., J. Nucl. Mater. 290 (2001) 196.
[59] H. Tsai et al., J. Nucl. Mater. 258–263 (1998) 1466.